FEBS Letters

FEBS PRESS science publishing by scientists

Binding and/or hydrolysis of purine-based nucleotides is not required for IM30 ring formation

Carmen Siebenaller[1], Lukas Schlösser[1], Benedikt Junglas[1,2,3], Martina Schmidt-Dengler[4], Dominik Jacob[4], Nadja Hellmann[1], Carsten Sachse[2,3], Mark Helm[4] and Dirk Schneider[1,5]

1 Department of Chemistry, Biochemistry, Johannes Gutenberg University Mainz, Germany
2 Ernst-Ruska Centre for Microscopy and Spectroscopy with Electrons (ER-C-3/Structural Biology), Forschungszentrum Jülich, Germany
3 JuStruct: Jülich Center for Structural Biology, Forschungszentrum Jülich, Germany
4 Institute for Pharmaceutical and Biomedical Sciences, Johannes Gutenberg University Mainz, Germany
5 Institute of Molecular Physiology, Johannes Gutenberg University Mainz, Germany

Correspondence
D. Schneider, Department of Chemistry, Johannes Gutenberg University Mainz, Hanns-Dieter-Hüsch-Weg 17, 55128 Mainz, Germany
Tel: (+49) 6131 39 25833
E-mail: Dirk.Schneider@uni-mainz.de

(Received 17 December 2020, revised 30 April 2021, accepted 20 May 2021, available online 21 June 2021)

doi:10.1002/1873-3468.14140

Edited by Peter Brzezinski

IM30, the inner membrane-associated protein of 30 kDa, is conserved in cyanobacteria and chloroplasts. Although its exact physiological function is still mysterious, IM30 is clearly essential for thylakoid membrane biogenesis and/or dynamics. Recently, a cryptic IM30 GTPase activity has been reported, albeit thus far no physiological function has been attributed to this. Yet, it is still possible that GTP binding/hydrolysis affects formation of the prototypical large homo-oligomeric IM30 ring and rod structures. Here, we show that the *Synechocystis* sp. PCC 6803 IM30 protein in fact is an NTPase that hydrolyzes GTP and ATP, but not CTP or UTP, with about identical rates. While IM30 forms large oligomeric ring complexes, nucleotide binding and/or hydrolysis are clearly not required for ring formation.

Keywords: cyanobacteria; IM30; PspA; Synechocystis; thylakoid membrane; Vipp1

Introduction

The *inner membrane-associated protein of 30 kDa* (IM30), also known as the *vesicle-inducing protein in plastids 1* (Vipp1), is a member of the PspA/IM30 protein family. The protein is conserved and essential in cyanobacteria and chloroplasts [1–3]. Depletion of IM30 in cyanobacteria leads to drastically impaired formation of thylakoid membranes (TMs), accompanied by a reduced photosynthetic activity [1,4–6]. Similar, but not entirely conclusive results have been reported for chloroplasts of *Arabidopsis thaliana* and *Chlamydomonas rheinhardtii* [3,7]. All results indicate a role of IM30 in TM dynamics, and IM30 appears to be crucially involved in two physiological processes: (a) membrane protection/repair and (b) membrane remodeling [8]. The membrane-protective activity of IM30 does not appear to be limited to TM-containing photosynthetic organisms, but is rather conserved in the entire PspA/IM30 family, as, for example, expression of IM30 complements the deficiencies of an *E. coli pspA* deletion strain [9,10]. In contrast, TM-specific functions of IM30 can likely not be accomplished by PspA [1,2,11,12].

A distinct structural feature of all PspA/IM30 family members is their intrinsic propensity to form large, homo-oligomeric ring/rod structures with masses > 1 MDa [8]. *In vitro* formation of rings and rods has been observed multiple times via electron microscopy [11,13–19] and atomic force microscopy (AFM) [20]. While *E. coli* PspA appears to form rings with a mainly constant diameter of ~ 20 nm [13], *Synechocystis* PspA and IM30 rings/rods were found to have varying diameters and symmetries [19,21]. Recently, the preliminary structures of homo-oligomeric cyanobacterial IM30 (*Synechocystis* sp., *Nostoc punctiforme* sp. PCC 73102) and PspA (*Synechocystis* sp. PCC 6803) have been made available [21–23]. PspA/IM30 monomers are mainly α-helical when organized into high molecular mass oligomers, with flexible

linkers connecting individual α-helical regions [21–24]. IM30 monomers are arranged horizontally to the ring axis, forming an interwoven, layer-like structure with 11–18 monomers per layer and 5–7 layers per ring [22–24]. In contrast to the homo-oligomer, the structure of membrane-bound IM30 is currently enigmatic. IM30 binds to thylakoid membranes *in vivo* [25,26] as well as to negatively charged model membranes *in vitro* [27–30]. Recently, upon membrane binding, dissociation of IM30 rings into partly unfolded monomers and subsequent formation of a membrane surface-covering carpet structure has been observed [20]. Thus, monomer adhesion to the membrane surface appears to be thermodynamically favored over ring formation. As the IM30 membrane-binding propensity is enhanced at acidic conditions, IM30 potentially binds specifically to stressed TM regions via sensing proton leakage followed by ring dissociation and formation of the membrane-protecting carpet [31]. Yet, IM30 is also able to trigger fusion of TM-mimicking liposomes *in vitro* when Mg^{2+} is present [27]. In fact, Mg^{2+} binding leads to a rearrangement of the oligomeric IM30 structure [29], which potentially switches the IM30 function from membrane protection to membrane remodeling.

wRecently, GTP binding and hydrolysis were observed for the IM30 proteins of *Arabidopsis thaliana* and *Synechocystis* sp. PCC 6803, although IM30 does not contain any canonical domains or motifs involved in GTP binding [32,33]. While GTP binding and/or hydrolysis do not seem to decisively regulate membrane interactions or the membrane remodeling activity of IM30 [32], it is still possible that GTP binding and/or hydrolysis might affect formation of IM30 rings. Actually, based on the identification of a stably bound nucleotide in oligomeric IM30, it has been suggested that ATP binding and/or hydrolysis are crucial for the formation of IM30 rings budding off from membrane surfaces [22].

In the present study, we show that *Syn*IM30 rings self-assemble in complete absence of nucleotides, and thus, nucleotide binding or hydrolysis do not trigger ring formation. Yet, *Syn*IM30 rings are able to hydrolyze ATP and GTP at about similar rates, but not CTP or UTP, and thus, IM30 in fact specifically binds and hydrolyzes purine-based nucleotides.

Experimental procedures

Cloning, expression, and purification of IM30

Construction of the plasmid used for expression of His-tagged wt *Syn*IM30 (pRSET IM30 wt) was described in detail previously [4], and construction of the plasmid used for expression of the IM30 FERM_EE mutant (E83A, E84A, F168A, E169A, R170A, M171A) is described in ref. [32].

IM30 of *Synechocystis* sp. PCC 6803 (*Syn*IM30 wt and FERM_EE) was heterologously expressed in *E. coli* BL21 DE3 and purified as described in detail earlier [16]. In short, after expression, cells were lysed via sonification in 50 mM Na-phosphate buffer (300 mM NaCl, 20 mM imidazole, pH 7.6). Cell debris was removed by centrifugation, and the supernatant was applied to a Ni^{2+}-NTA affinity column. The column was washed with increasing concentrations of imidazole (20/50/100 mM; 50 mM Na-phosphate, 300 mM NaCl, pH 7.6) and finally eluted with 500 mM imidazole (Na-phosphate, 300 mM NaCl, pH 7.6). The buffer was exchanged for 20 mM HEPES (pH 7.6) by gel filtration (Sephadex G25 or Superose 12). Where necessary, the protein solution was concentrated using an Amicon Ultra Centrifugal filter unit (MWCO 30 kDa, regenerated cellulose membrane). The protein concentration was determined via a Bradford assay using BSA as a standard. For denaturation, 6 M urea was added to the lysis buffer and the cell extract was incubated in 6 M urea for 4 h at 4 °C. Subsequently, upon loading the sample onto the affinity column, the sample was washed multiple times with buffer containing 20 mM imidazole plus 6 M urea. For refolding on the column, the subsequent washing steps (compare above) and the elution were performed using urea-free buffer, as used in case of purification under native conditions. For analysis of the NTPase activity, the purification was performed in HEPES buffer instead of phosphate buffer as described before [32]. In this case, the protein solutions were stored in 1 : 1 (v/v) glycerol at −20 °C.

Size exclusion chromatography

The size of *Syn*IM30 oligomers was analyzed using an ÄKTA basic system (GE Healthcare, Freiburg, Germany) with a Superose12 10/300 GL column (GE Healthcare) equilibrated with 20 mM HEPES (pH 7.6) at 8 °C. Protein elution was followed via monitoring the absorbance at 280 nm. The column was calibrated using standards of known size (blue dextran > 2000 kDa, ferritin (440 kDa), β-amylase (200 kDa), aldolase (158 kDa), conalbumin (75 kDa), ovalbumin (44 kDa), carbonic anhydrase (29 kDa), and cytochrome c oxidase (16.4 kDa)).

Circular dichroism spectroscopy

Circular dichroism (CD) spectra were measured using a JASCO J815 CD spectrometer (JASCO Corporation,

Tokyo, Japan). With purified native and the refolded protein, spectra ranging from 200 to 260 nm were recorded at 20 °C with a scan rate of 100 nm·min^{-1}, 1 nm steps, and 1 s data integration time. When urea-denatured protein was analyzed, spectra were measured from 210 to 260 nm. Each sample contained 0.1 mg·mL^{-1} *Syn*IM30 in 10 mM HEPES buffer (pH 7.6) or 10 mM HEPES buffer and 6 M urea (pH 7.6). For each sample, three spectra were averaged and smoothened by the JASCO software package (Savitzky–Golay filter), if necessary.

Electron microscopy

For negative-staining electron microscopy, 3 µL sample was applied to glow-discharged (PELCO easiGlow Glow Discharger, Ted Pella Inc., Redding, CA, USA) continuous carbon grids (CF-300 Cu, Electron Microscopy Sciences, Hatfield, PA, USA). The sample was incubated on the grid for 1 min. Then, the grid was side-blotted on filter paper, washed with 3 µL water, and stained with 3 µL 2% uranyl acetate for 30 s and air-dried. The grids were imaged with a 120 kV Talos L120C electron microscope (Thermo Fisher Scientific/FEI, Hillsboro, OR, USA) equipped with a CETA camera at a pixel size of 4.06 Å/pix at an underfocus of 1.0–2.5 µm.

Malachite Green assay

0.1 µM *Syn*IM30 was mixed with 0.5 mM of GTP, ATP, CTP, or UTP and Mg^{2+} (2.5 mM) in 20 mM Hepes (pH 7.6) and incubated for 30 min at 37 °C. 200 µL of this sample was transferred to a 96-well plate, mixed with 50 µL of the malachite green reaction mixture ('Gold mix', PiColorLock Gold Phosphate Detection Kit, Innova Biosciences, Cambridge, UK) and incubated for 5 min at RT. Finally, 20 µL of 'stabilizer' was added. Absorbance at 635 nm was measured using an OMEGA FLUOstar Platereader (BMG Labtech, Ortenberg, Germany). Buffer blank (including the respective NTP concentration) absorbance was subtracted, and the concentration of released phosphate was determined by linear regression from a phosphate standard curve.

LC-MS analysis of extracted nucleoside phosphates in negative ion mode

25 µM *Syn*IM30 was incubated for 30 min in methanol (final concentration 80%) to denature the protein. Protein denaturation was verified *via* CD spectroscopy. Denaturation dismantles the potential nucleotide-binding site and releases any bound nucleotide. The precipitated protein was removed by centrifugation at 16 000 ***g*** and 4 °C for 15 min. The supernatant containing any beforehand protein-bound substances was collected, dried in a SpeedVac (vacuum centrifuge, Eppendorf, Hamburg, Germany), and finally resuspended in water.

For separation and subsequent mass-spectrometric analysis of the nucleotide solutions, a chromatographic approach from Xing *et al.* was adapted [34]. Sample amounts corresponding to 500 pmol initial protein were injected onto a Hypercarb column (5 µm, 100 × 2.1 mm) (Thermo Scientific, Waltham, MA, USA), and the column oven was set to 35 °C. Mobile phase A (MPA) consisted of 50 mM ammonium acetate and 0.1% diethylamine in water (pH = 9) and mobile phase B (MPB) of pure, LC-MS grade ACN. At a flow rate of 0.5 mL·min^{-1}, the following gradient was run: 5% MPB from 0 to 2 min, 5–20% MPB from 2 to 8 min, 20–90% MPB from 8 to 14 min, 90% MPB from 14 to 15 min, 90–5% MPB from 15 to 17 min, and 5% MPB from 17 to 22 min. Mass spectrometric analyses of the negatively charged ions were conducted using an Agilent 6460 QQQ mass spectrometer in the dynamic multiple reaction monitoring mode (dMRM). This allows monitoring a specific fragmentation reaction at a given retention time. The selected mass transitions and retention time windows are displayed in Table 1. Ion source parameters were set as followed: gas temperature 350 °C, gas flow 8 L·min^{-1}, nebulizer pressure 50 psi, sheath gas temperature 350 °C, sheath gas flow 2 L·min^{-1}, capillary voltage −3500 V.

Table 1. QQQ parameters for the detection of NTPs.

Compound name	Precursor ion	Product ion	Fragmentor	Collision energy	Cell accelerator voltage	Ret. time (min)	Delta ret. time
ATP	506	159	95	29	5	9.3	4
ADP	426	79	100	40	5	9.1	4
GTP	522.3	424	105	17	5	9	4
GDP	442	79	105	40	5	9	4

Results and Discussion

IM30 hydrolyzes purine-based, but not pyrimidine-based nucleotides

As shown before, IM30 oligomers of *Synechocystis* and *Arabidopsis* hydrolyze GTP reaching a P_i release rate of about 20 μM at 2 μg/100 μL protein concentration [32,33]. To gain further insights into the specificity and (potential) function of GTP binding, we at first analyzed the nucleotide binding/hydrolysis specificity and tested whether IM30 of the cyanobacterium *Synechocystis* sp. PCC 6803 (*Syn*IM30) is also able to hydrolyze other nucleoside triphosphates (NTPs). Therefore, we used a well-established malachite green-based assay to analyze the apparent NTPase activity of *Syn*IM30. As a negative control, we used the IM30 mutant *Syn*IM30 FERM_EE, which does not hydrolyze GTP, as shown recently [32]. Based on the now available IM30 structure, this is obvious, as this mutant does not form higher-ordered oligomers anymore, and oligomerization is required for nucleotide binding as further discussed below [22].

When the purity of IM30 wt was analyzed via SDS-PAGE (Fig. 1A), no other proteins were detected (Fig. 1A). While the purified *Syn*IM30 wt protein, but not the mutant, clearly hydrolyzes the purine-based nucleotides GTP and ATP to a similar extent, very little activity was observed when the pyrimidine-based CTP or UTP were added instead (Fig. 1B). This implies that IM30 specifically hydrolyzes purine-based, but not pyrimidine-based nucleotides, and IM30 is in fact not a GTPase but an NTPase, hydrolyzing GTP and ATP with about identical rates (Fig. 1B). This observation is in excellent agreement with the initially observed GTP-hydrolyzing activity of *Syn*IM30 [32] and the now observed binding of ADP to IM30 rings [22,24].

Thus far, solely interaction between defined IM30 side chains with the phosphate groups of the NTP has been suggested to be involved in nucleotide binding [22]. Our results now clearly indicate that also the bases are decisive for the interaction with IM30, and the putative nucleotide-binding pocket appears to specifically bind the larger purine-heterocycle of NTPs.

Substrate promiscuity is not common but reported for several ATP/GTPases, and, for example the predicted GTP-binding protein HflX exhibits a GTPase as well as an ATPase activity, albeit the activities were not identical [35]. Similarly, the YchF subfamily, a unique subgroup of the Obg family of P-loop GTPases, binds both, GTP and ATP [36]. It has been hypothesized that during the evolution of the GTPase superclass from a primordial GTPase, the activity of some proteins has switched to an ATPase activity on several independent occasions [37,38]. Nevertheless, all these proteins do contain canonical nucleotide-binding motifs in their sequence, in contrast to IM30.

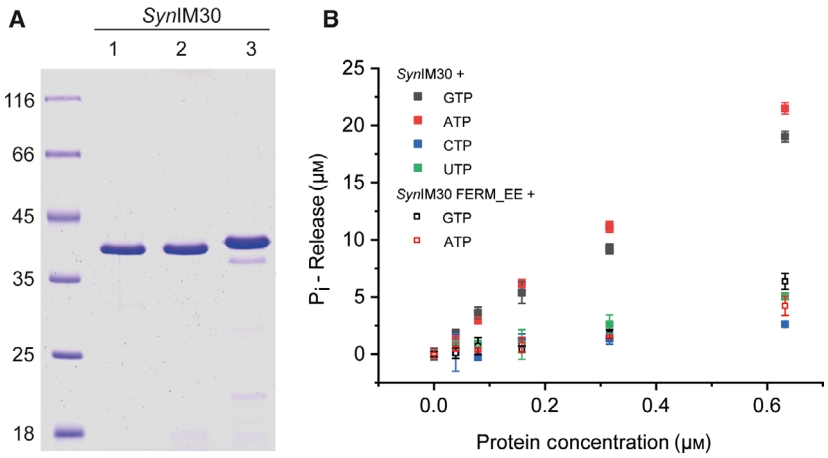

Fig. 1. IM30 specifically hydrolyzes purine-based nucleotides. (A) SDS/PAGE analysis of heterologously expressed and purified IM30 wt (lane 1), of *in vitro* refolded IM30 wt (lane 2), as well as of purified IM30 FERM_EE (lane 3). The wt protein was electrophoretically pure, whereas we observed some small degradation products in case of IM30 FERM_EE. The molecular masses of the protein standard are given on the left. (B) The P_i release caused by increasing amounts of IM30 in presence of 0.5 mM GTP (black), ATP (red), CTP (blue), or UTP (green) and 2.5 mM Mg^{2+} after incubation for 30 min at 37 °C was measured using a malachite green-based assay. Only minor release of P_i was detected in the negative control (IM30 FERM_EE) (black squares with holes: GTP, red squares with holes: ATP). When the wt protein was analyzed, exclusively in presence of the purine-based nucleotides GTP or ATP, a significant amount of P_i was released (error bars represent SD, $n = 3$).

Compared to most other GTP-hydrolyzing enzymes, the activity, as well as the GTP-binding affinity of IM30, is relatively low [32]. Still, the rates observed previously [32] and here, as well as described for the isolated *Arabidopsis* IM30 [33], are at least 10-fold higher than the putative activity reported very recently for the wt and mutated *Synechocystis* proteins [22]. The rather low NTPase activity of IM30 might be due to a very slow k_{off} rate for ADP and GDP from the putative binding pocket, resulting in a very slow regeneration of the IM30 protein. This assumption is supported by the observation that after the addition of ATP, a stably bound ADP was detected in the cryo-EM structure of IM30 even after further purification steps [22]. Tight binding of ADP/GDP is rather uncommon for classical GTP/ATPases, but clarifies the negative result of an enzyme-coupled GTPase assay that is based on the detection of free GDP [32].

IM30 nucleotide binding is not required for IM30 ring formation

The structure of oligomeric IM30 was recently analyzed via cryo-EM single-particle analysis [22]. In the reported structure, a stably bound ADP in a unique nucleotide-binding site has been detected, when the protein was incubated in ATP solutions prior to structural analyses [22].

When we analyzed the presence of nucleotides in our protein sample (500 pmol protein) that was purified without an ATP-including washing step, we did not observe any measurable concentrations of the nucleotides ADP/ATP or GDP/GTP (Fig. 2A,B). The lower limit of quantification was 10 pmol, resulting in a maximum nucleotide-bound protein fraction of not more than 2%. Thus, we exclude that endogenous nucleotides from the *E. coli* cells were co-purified with the protein.

Next, we analyzed the structure of the nucleotide-free IM30 protein by negative-staining electron microscopy. Here, we observed the characteristic IM30 ring structures as well as some rod-like structures (Fig. 2C), as observed multiple times before for purified IM30 [16,19,29,30,39,40]. Thus, nucleotide binding clearly is not crucial for stabilizing the IM30 ring structures.

Yet, this does not allow to finally exclude that ATP (or GTP)-binding and/or hydrolysis might be a crucial (initial) step in IM30 ring formation, as this might already take place in *E. coli* during protein expression. However, we have shown previously that IM30 elutes as monomers or lower ordered oligomers from the Ni-NTA matrix, which (re)assemble and form rings/rods likely only later on after the purification process in complete absence of nucleotides [19]. Noteworthy, when IM30 is not assembled in higher-ordered oligomers, about half of the protein is unfolded [20]. Furthermore, also the recently published structure of *Syn*IM30 [22] was solved using a protein that was purified when its N terminus was fused to a chitin-binding domain. The mature IM30 protein was released only after protease treatment [22]. As the protein's N terminus is embedded within the narrow center of an IM30 ring [22], likely monomers or smaller oligomers were purified, which assembled to the final ring structures only after removal of the fusion domain.

Nevertheless, to further test whether ATP/GTP (or ADP/GDP) is required for IM30 ring assembly, we completely denatured IM30 prior to protein purification via addition of 6 M urea. As shown before, IM30 has no α-helical structure in 6 M urea solutions, resulting in the loss of any potential nucleotide-binding site [29] (Fig. 3A). The Ni^{2+}-NTA-bound denatured protein was washed multiple times with 6 M urea-containing buffer to remove any potentially co-purified substances, such as proteins, lipids, ions, or nucleotides. Subsequently, the protein was refolded on the column by washing with urea-free buffer. Note that the overall secondary structure of renatured IM30 did not differ from the secondary structure of IM30 purified under native conditions (Fig. 3A), indicating correct refolding of secondary structure elements of IM30 in absence of nucleotides. As the monomeric protein is partly unfolded [20], this already indicated formation of higher-ordered structures where the IM30 monomer is largely α-helical. Furthermore, when the refolded protein was analyzed via size-exclusion chromatography, solely high molecular weight oligomers were detected, but no smaller oligomers or monomers (Fig. 3B), and these high molecular weight species were identified by negative-staining EM as the prototypical IM30 ring and rod structures (Fig. 3C). As expected, we did not detect any nucleotides in our urea-treated and refolded protein samples, when analyzed by LC/MS as described (Fig. S1).

Thus, IM30 is unequivocally self-assembling and oligomerizing into ring structures without nucleotide binding and/or hydrolysis.

The ADP molecules observed in the cryo-EM structure most likely are a result of the ATP-including washing step that was applied during purification of *Syn*IM30 [22]. It is well possible that ATP or GTP binding slightly distorts the IM30 structure and/or ATP/GTP binds solely to slightly distorted protein regions. In fact, the putative nucleotide-binding site is formed by different regions of three different IM30

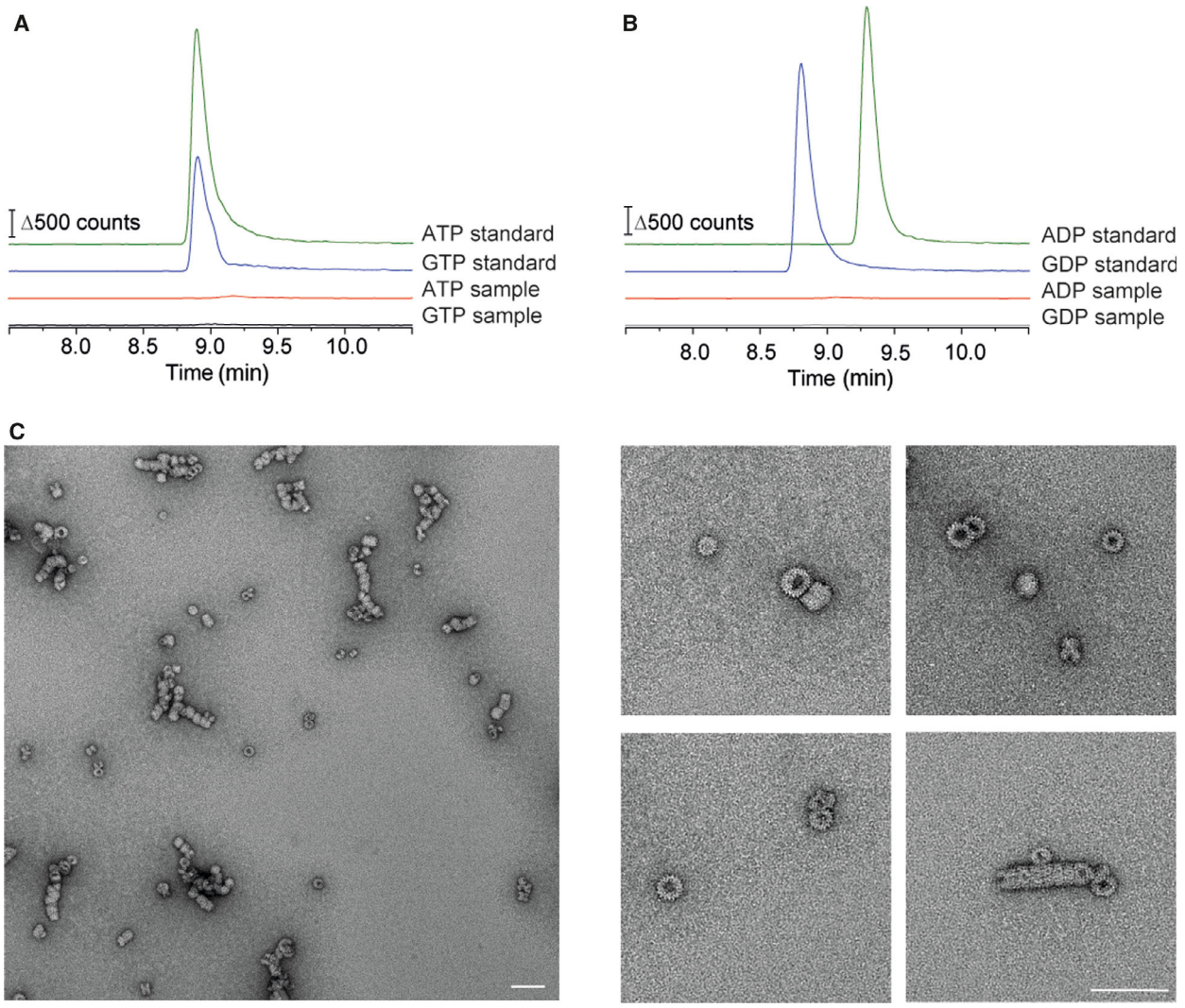

Fig. 2. IM30 assembles into rings in complete absence of nucleotides. (A, B) Extracted ion chromatograms (EIC) of specific mass transitions for (A) ATP (*m/z* 506 → 159) and GTP (*m/z* 522,3 → 442) and for (B) ADP (*m/z* 426 → 79) and GDP (*m/z* 442 → 79) from the wt IM30 sample (500 pmol) and nucleotide standards (200 pmol) as a control. C: Electron microscopy of purified IM30 wt in absence of nucleotides. Scale bars represent 100 nm.

monomers, two from layer 1 and one from layer 2. Yet, due to the basket-like structure of IM30 rings, the structure of IM30 monomers is somewhat distorted in the first three layers of a ring [22]. When natively folded *Syn*PspA was compared to *in vitro* refolded *Syn*PspA, formation of the prototypical rod structures was observed, but the refolded rods appeared to exhibit extended lengths and even looked more regular compared to the natively folded protein [21]. Due to these observations, we next tested whether the *in vitro* refolded IM30 rings still have a GTP/ATP-hydrolyzing activity. As can be seen in Fig. S2, the prototypical IM30 rings do not show any significant ATP or GTP-hydrolyzing activity anymore after *in vitro* folding. While the here measured values (background) are still higher than the values reported recently for the *Syn*IM30 wt protein [22], the refolded protein releases P_i at similar low rates as measured with the negative control. Thus, the nucleotide-binding site of IM30 likely might be slightly differently structured after refolding, which does, however, neither lead to overall misfolding of the secondary structure (Fig. 3A), nor to a disturbed oligomerization and ring formation (Fig. 3B,C). This again indicates that nucleotide binding/hydrolysis is not relevant for formation and/or stabilization of the prototypical IM30 ring structures, despite the localization of the proposed binding site at the interface of three monomers inside the ring [22].

In fact, based on a recent *de novo* protein design study, it has been discussed that some level of ATP binding and ATPase activity is not unusual in protein sequence space, and an ATP-hydrolyzing activity can be observed for proteins that differ substantially from naturally occurring ATPases [41]. Thus, determining a low ATP/GTP-hydrolyzing activity, as, for example, observed with IM30, might not be uncommon. Yet, the apparent lack of structural diversity among naturally occurring ATPases (and GTPases) strongly indicates that, while binding and catalysis can be accomplished by alternative sequences and structures, the energy gained via NTP hydrolysis might not be properly transmitted into a biological activity by non-canonical binding sites.

Conclusion

We here show that *Syn*IM30 rings can hydrolyze ATP and GTP at about identical rates, but not CTP or UTP. The absence of nucleotides does not influence oligomerization of IM30 monomers into ring structures, and the negative-staining EM analyses clearly showed formation of typical ring- and rod structures (Fig. 2C). Furthermore, IM30 prototypical rings do also spontaneously assemble from completely denatured protein in complete

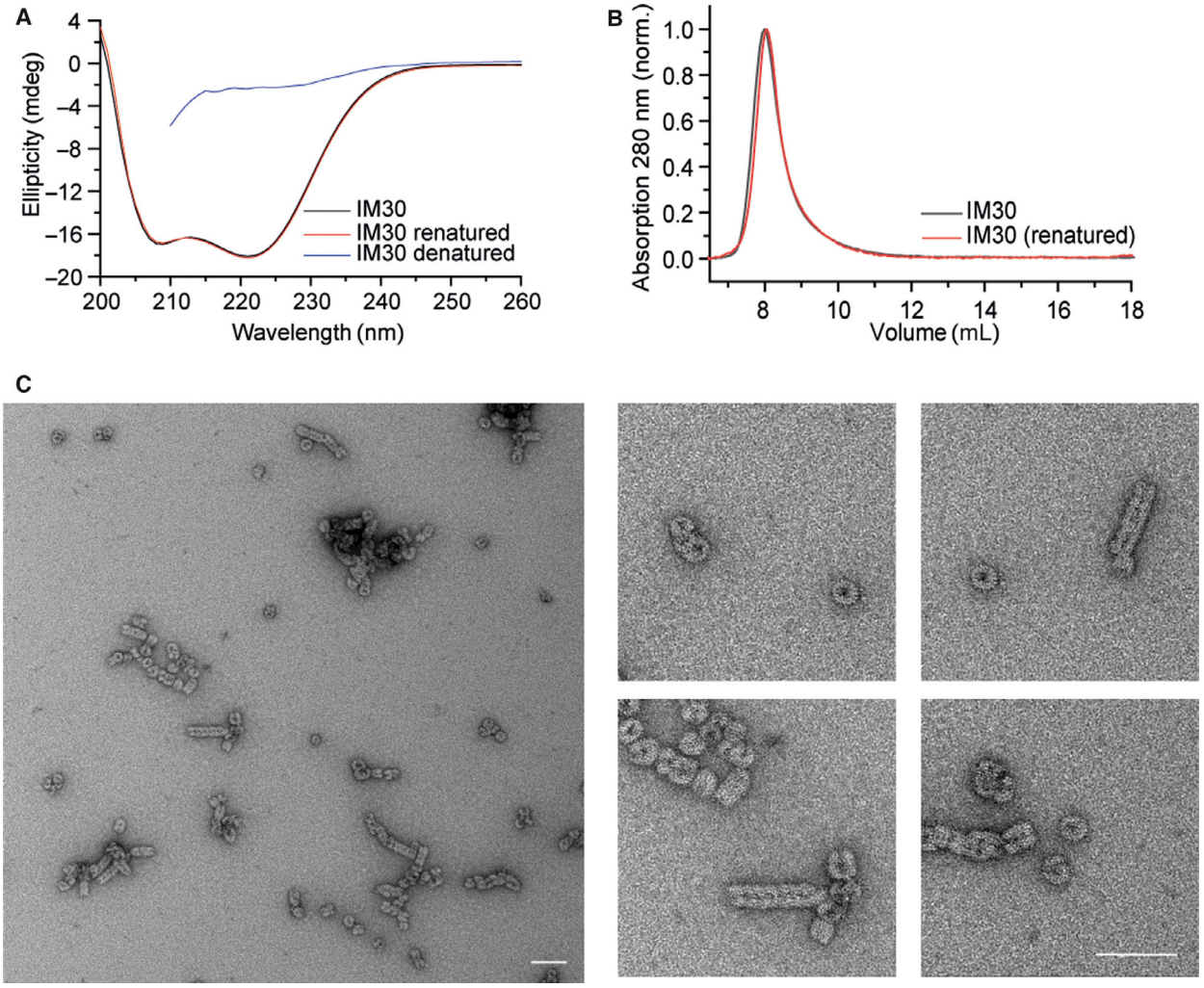

Fig. 3. IM30 self-assembles into ring-like structures. (A) CD spectra of IM30 purified under standard conditions or after renaturation were measured from 200 to 260 nm. The spectra do not differ, indicating proper folding of the secondary structure of the renatured sample. The spectra were smoothened using a Savitzky-Golay filter. $n = 3$, no error bars are shown. When the secondary structure of IM30 was analyzed after urea denaturation, the spectra indicated complete unfolding of the protein. (B) The oligomeric state of IM30 was monitored by SEC (Superose 12 10/300 GL column). Both, IM30 wt purified under standards conditions (black) and IM30 wt purified under denaturing conditions and refolded (red) eluted in the void volume (> 300 kDa). (C) IM30 purified under denaturing conditions was analyzed by negative-staining EM. Ring as well as some rod structures were observed. The scale bar represents 100 nm.

absence of nucleotides (Fig. 3C). As a putative ADP-binding pocket has been detected between two layers of an IM30 ring, which involves interactions of a single nucleotide with three different IM30 monomers [22,24], the oligomeric structure of IM30 clearly is a prerequisite for nucleotide binding. This is perfectly in line with the observation that the oligomerization-inactive IM30 mutant had no GTP-hydrolyzing activity [32] (Fig. 1B). This consequently implies that nucleotide binding and (potentially) hydrolysis can physiologically only be relevant (if at all), when the large oligomeric complex has already formed. Clearly, membrane interaction destabilizes IM30 rings resulting in formation of an IM30 carpet structure on the membrane surface [20], and thus, ring dissociation and IM30 monomer-membrane interactions are thermodynamically favored over ring formation at membrane surfaces. Furthermore, the presence of GTP tends to decrease the thermal stability of IM30 rings [32], and thus, nucleotide binding does not stabilize, but destabilize an IM30 ring structure. These observations do not support the idea that IM30 ring formation is initiated on membrane surfaces by ATP/GTP binding and/or hydrolysis, but rather suggests a nucleotide-independent mechanism for IM30 oligomerization. Thus, as nucleotide binding to and/or hydrolysis by IM30 neither decisively regulates the IM30 oligomeric structure nor membrane interactions [32], we suggest that IM30 nucleotide hydrolysis may not play a crucial role in the function of membrane repair based on the current knowledge. Nevertheless, the residues identified to be involved in nucleotide binding in the ATP-washed sample appear to establish important contacts within the IM30 oligomer or with other factors, as mutation of these residues results in an impaired *in vivo* activity of IM30 [22]. Future information on the *in vivo* IM30 structure might be of help to unravel a potential *in vivo* function of the cryptic nucleotide binding/hydrolysis activity.

Acknowledgements

This work was funded by the Max-Planck Graduate Center at the Max-Planck Institutes and the University of Mainz and a DFG Grant HE 3397/13-2 to M.H.

Conflict of interest

The authors declare that they do not have any competing conflict of interest.

Author contributions

MH, CSa, and DS conceived and supervised the study. CSi, LSBJ, MS, and DJ performed the experiments. CSi, LS, BJ, MS, DJ, and NH analyzed the data. All authors wrote the manuscript.

Data accessibility

The data that support the findings of this study are available in Figs 1–3 and the supplementary material of this article.

References

1 Westphal S, Heins L, Soll J and Vothknecht UC (2001) Vipp1 deletion mutant of Synechocystis: a connection between bacterial phage shock and thylakoid biogenesis? *Proc Natl Acad Sci USA* **98**, 4243–4248.
2 Vothknecht UC, Otters S, Hennig R and Schneider D (2012) Vipp1: a very important protein in plastids?! *J Exp Bot* **63**, 1699–1712.
3 Kroll D, Meierhoff K, Bechtold N, Kinoshita M, Westphal S, Vothknecht UC, Soll J and Westhoff P (2001) VIPP1, a nuclear gene of *Arabidopsis thaliana* essential for thylakoid membrane formation. *Proc Natl Acad Sci USA* **98**, 4238–4242.
4 Fuhrmann E, Gathmann S, Rupprecht E, Golecki J and Schneider D (2009) Thylakoid membrane reduction affects the photosystem stoichiometry in the cyanobacterium *Synechocystis* sp. PCC 6803. *Plant Physiol* **149**, 735–744.
5 Gao H and Xu X (2009) Depletion of Vipp1 in *Synechocystis* sp. PCC 6803 affects photosynthetic activity before the loss of thylakoid membranes. *FEMS Microbiol Lett* **292**, 63–70.
6 Zhang S, Shen G, Li Z, Golbeck JH and Bryant DA (2014) Vipp1 is essential for the biogenesis of Photosystem I but not thylakoid membranes in *Synechococcus* sp. PCC 7002. *J Biol Chem* **289**, 15904–15914.
7 Nordhues A, Schottler MA, Unger A-K, Geimer S, Schonfelder S, Schmollinger S, Rutgers M, Finazzi G, Soppa B, Sommer F *et al.* (2012) Evidence for a role of VIPP1 in the structural organization of the photosynthetic apparatus in Chlamydomonas. *Plant Cell* **24**, 637–659.
8 Siebenaller C, Junglas B and Schneider D (2019) Functional implications of multiple IM30 oligomeric states. *Front Plant Sci* **10**, 1–11.
9 DeLisa MP, Lee P, Palmer T and Georgiou G (2004) Phage shock protein PspA of *Escherichia coli* relieves saturation of protein export via the Tat Pathway. *J Bacteriol* **186**, 366–373.
10 Zhang L, Kato Y, Otters S, Vothknecht UC and Sakamoto W (2012) Essential role of VIPP1 in chloroplast envelope maintenance in Arabidopsis. *Plant Cell* **24**, 3695–3707.
11 Aseeva E, Ossenbühl F, Eichacker LA, Wanner G, Soll J and Vothknecht UC (2004) Complex formation of

Vipp1 depends on its alpha-helical PspA-like domain. *J Biol Chem* **279**, 35535–35541.
12 Bultema JB, Fuhrmann E, Boekema EJ and Schneider D (2010) Vipp1 and PspA. *Commun Integr Biol* **3**, 162–165.
13 Hankamer BD, Elderkin SL, Buck M and Nield J (2004) Organization of the AAA+ adaptor protein PspA is an oligomeric ring. *J Biol Chem* **279**, 8862–8866.
14 Wolf D, Kalamorz F, Wecke T, Juszczak A, Mäder U, Homuth G, Jordan S, Kirstein J, Hoppert M, Voigt B *et al*. (2010) In-depth profiling of the LiaR response of *Bacillus subtilis*. *J Bacteriol* **192**, 4680–4693.
15 Liu C, Willmund F, Golecki JR, Cacace S, Heß B, Markert C and Schroda M (2007) The chloroplast HSP70B-CDJ2-CGE1 chaperones catalyse assembly and disassembly of VIPP1 oligomers in Chlamydomonas. *Plant J* **50**, 265–277.
16 Fuhrmann E, Bultema JB, Kahmann U, Rupprecht E, Boekema EJ and Schneider D (2009) The vesicle-inducing protein 1 from *Synechocystis* sp. PCC 6803 organizes into diverse higher-ordered ring structures. *Mol Biol Cell* **20**, 4620–4628.
17 Gao F, Wang W, Zhang W and Liu C (2015) α-Helical domains affecting the oligomerization of Vipp1 and its interaction with Hsp70/DnaK in *Chlamydomonas*. *Biochemistry* **54**, 4877–4889.
18 Male AL, Oyston PCF and Tavassoli A (2014) Self-assembly of *Escherichia coli* phage shock protein A. *Adv Microbiol* **04**, 353–359.
19 Saur M, Hennig R, Young P, Rusitzka K, Hellmann N, Heidrich J, Morgner N, Markl J and Schneider D (2017) A Janus-faced IM30 ring involved in thylakoid membrane fusion is assembled from IM30 tetramers. *Structure* **25**, 1380–1390.e5.
20 Junglas B, Orru R, Axt A, Siebenaller C, Steinchen W, Heidrich J, Hellmich UA, Hellmann N, Wolf E, Weber SAL *et al*. (2020) IM30 IDPs form a membrane-protective carpet upon super-complex disassembly. *Commun Biol* **3**, 595.
21 Junglas B, Huber ST, Heidler T, Schlösser L, Mann D, Hennig R, Clarke M, Hellmann N, Schneider D and Sachse C (2021) PspA adopts an ESCRT-III-like fold and remodels bacterial membranes. *bioRxiv* 2020.09.23.309765.
22 Kumar Gupta T, Klumpe S, Gries K, Heinz S, Wietrzynski W, Ohnishi N, Niemeyer J, Schaffer M, Rast A, Strauss M *et al*. (2020) Structural basis for VIPP1 oligomerization and maintenance of thylakoid membrane integrity. *bioRxiv* 2020.08.11.243204.
23 Liu J, Tassinari M, Souza DP, Naskar S, Noel JK, Bohuszewicz O, Buck M, Williams TA, Baum B and Low HH (2020) Bacterial Vipp1 and PspA are members of the ancient ESCRT-III membrane-remodelling superfamily. *bioRxiv* 2020.08.13.249979.
24 McCullough J and Sundquist WI (2020) Membrane remodeling: ESCRT-III filaments as molecular garrotes. *Curr Biol* **30**, R1425–R1428.
25 Bryan SJ, Burroughs NJ, Shevela D, Yu J, Rupprecht E, Liu LN, Mastroianni G, Xue Q, Llorente-Garcia I, Leake MC *et al*. (2014) Localisation and interactions of the Vipp1 protein in cyanobacteria. *Mol Microbiol* **94**, 1179–1195.
26 Zhang L, Kondo H, Kamikubo H, Kataoka M and Sakamoto W (2016) VIPP1 has a disordered C-terminal tail necessary for protecting photosynthetic membranes against stress. *Plant Physiol* **171**, 1983–1995.
27 Hennig R, Heidrich J, Saur M, Schmüser L, Roeters SJ, Hellmann N, Woutersen S, Bonn M, Weidner T, Markl J *et al*. (2015) IM30 triggers membrane fusion in cyanobacteria and chloroplasts. *Nat Commun* **6**, 7018.
28 McDonald C, Jovanovic G, Ces O and Buck M (2015) Membrane stored curvature elastic stress modulates recruitment of maintenance proteins pspa and vipp1. *MBio* **6**, e01188-15.
29 Heidrich J, Junglas B, Grytsyk N, Hellmann N, Rusitzka K, Gebauer W, Markl J, Hellwig P and Schneider D (2018) Mg2+ binding triggers rearrangement of the IM30 ring structure, resulting in augmented exposure of hydrophobic surfaces competent for membrane binding. *J Biol Chem* **293**, 8230–8241.
30 Thurotte A and Schneider D (2019) The fusion activity of IM30 rings involves controlled unmasking of the fusogenic core. *Front Plant Sci* **10**, 108.
31 Siebenaller C, Junglas B, Lehmann A, Hellmann N and Schneider D (2020) Proton leakage is sensed by IM30 and activates IM30-triggered membrane fusion. *Int J Mol Sci* **21**, 4530.
32 Junglas B, Siebenaller C, Schlösser L, Hellmann N and Schneider D (2020) GTP hydrolysis by Synechocystis IM30 does not decisively affect its membrane remodeling activity. *Sci Rep* **10**, 1–14.
33 Ohnishi N, Zhang L and Sakamoto W (2018) VIPP1 involved in chloroplast membrane integrity has GTPase activity in vitro. *Plant Physiol* **177**, 328–338.
34 Xing J, Apedo A, Tymiak A and Zhao N (2004) Liquid chromatographic analysis of nucleosides and their mono-, di- and triphosphates using porous graphitic carbon stationary phase coupled with electrospray mass spectrometry. *Rapid Commun Mass Spectrom* **18**, 1599–1606.
35 Dutta D, Bandyopadhyay K, Datta AB, Sardesai AA and Parrack P (2009) Properties of HflX, an enigmatic protein from escherichia coli. *J Bacteriol* **191**, 2307–2314.
36 Cheung MY, Li X, Miao R, Fong YH, Li KP, Yung YL, Yu MH, Wong KB, Chen Z and Lam HM (2016) ATP binding by the P-loop NTPase OsYchF1 (an unconventional G protein) contributes to biotic but not abiotic stress responses. *Proc Natl Acad Sci USA* **113**, 2648–2653.

37 Leipe DD, Koonin EV and Aravind L (2004) STAND, a class of P-loop NTPases including animal and plant regulators of programmed cell death: Multiple, complex domain architectures, unusual phyletic patterns, and evolution by horizontal gene transfer. *J Mol Biol* **343**, 1–28.
38 Leipe DD, Wolf YI, Koonin EV and Aravind L (2002) Classification and evolution of P-loop GTPases and related ATPases. *J Mol Biol* **317**, 41–72.
39 Heidrich J, Wulf V, Hennig R, Saur M, Markl J, Sönnichsen C and Schneider D (2016) Organization into higher ordered ring structures counteracts membrane binding of IM30, a protein associated with inner membranes in chloroplasts and cyanobacteria. *J Biol Chem* **291**, 14954–14962.
40 Hennig R, West A, Debus M, Saur M, Markl J, Sachs JN and Schneider D (2017) The IM30/Vipp1 C-terminus associates with the lipid bilayer and modulates membrane fusion. *Biochim Biophys Acta Bioenerg* **1858**, 126–136.
41 Wang MS and Hecht MH (2020) A completely de novo ATPase from combinatorial protein design. *J Am Chem Soc* **142**, 15230–15234.

Supporting information

Additional supporting information may be found online in the Supporting Information section at the end of the article.

Fig. S1. Renatured IM30 does not bind any nucleotides.

Fig. S2. Renatured IM30 does not hydrolyze ATP or GTP.